VI International Conference on Textile Composites and Inflatable Structures
STRUCTURAL MEMBRANES 2015
E. Oñate, K.-U.Bletzinger, and B. Kröplin (Eds)

BENDING-ACTIVATED TENSEGRITY

E. SCHLING[*], R. BARTHEL[*], A. IHDE[*], J. TUTSCH[*] AND S. HUTH[*]

[*]Chair of Structural Design (LT)
Department of Architecture
Technische Universität München (TUM)
Arcisstr. 21, 80333 Munich, Germany
e-mail: ls.barthel@tum.de - Web page: www.lt.ar.tum.de

Key words: tensegrity, membranes, active bending, FEM, form-finding, GRP

Summary. The symbiosis of tensegrity and active bending was studied in an experimental structure called "Form Follows Tension". This paper covers all aspects of the planning process, including design, analysis, simulation and method statement.

Figure 1: Installation 'Form Follows Tension' by Sebastian Huth (photo: Matthias Kestel)

1 INTRODUCTION

Tensegrity structures – originally investigated by R. B. Fuller and K. Snelson in the 1960s – have since fascinated both engineers and artists. Frei Otto already studied the combination of membranes and tensegrity, and it was later declared a new principle, "Textegrity", by

Meeß-Olsohn[5]. These hybrid structures show outstanding aesthetic qualities in their natural lightness and transparency. At the same time they offer efficient structural solutions by combining pure compression and tension elements.

The last few years have brought an increasing research interest in the field of Bending-Active Structures[3], which, in a similar way, merge the design of form and structure. Beyond constructional advantages, this design principle allows for the utilization of residual bending stresses, which can improve the structural performance.

The beauty of these principles – tensegrity, membranes and active bending – lies in their natural expression of form, resembling their inner stress distribution. The following case study aims to unite these principles in an aesthetic and structural symbiosis.

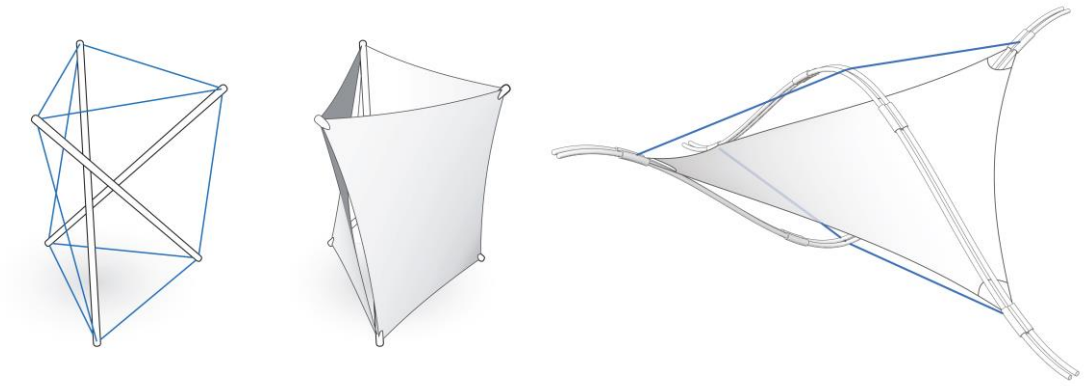

Figure 2: Tensegrity-, textegrity- and 'bending-activated tensegrity'- module

2 PRELIMINARY DESIGN

In the design studio, 'Experimental Structures', Sebastian Huth developed a modular structure comparable to the 'tensegrity double layer grid prototype' by R. Motro[6]. However, instead of pure compression, he introduced elastic elements. These 'active-bending'-rods can take on the desired, curved shape, carry the compression and introduce tension to the cables and membranes inside the structure (Fig. 1).

The basic module (Fig. 2) consists of two elastically bent spring-steels rods, which are positioned orthogonally, with their concave sides facing each other. A membrane is tied to their four outer points, while two cables connect the extremities of one arch to the center of the opposing arch[7]. The tensile stress inside the membranes and cables balances out and stabilizes the position of the steel rods.

These modules are replicated in an orthogonal planar grid. The elastic rods form interwoven sinus curves that never touch. Every intersection is fixed by a membrane and two sets of cables. This creates a closed tensegrity system in which all stresses are at equilibrium.

Huth built an installation consisting of 5 x 5 modules (Fig. 3) with nine inner modules, twelve edge modules and four corner modules. Inside the woven system, membranes and cables are attached tangentially to the bending rods, while along the edge, they are tied to the rods' extremities. This results in an asymmetric geometry and a decrease in tensile stress and stability at the edge and corner modules.

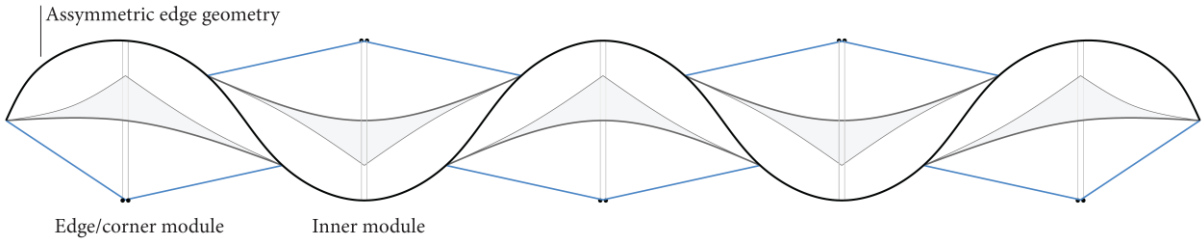

Figure 3: Section of 5 x 5 system showing the asymmetric edge condition

3 DESIGN DEVELOPMENT AND SCALE

The installation was redeveloped at a larger scale consisting of 2 x 2 modules (Fig. 4, 5) with the overall dimensions of approx. 6 x 6 m. The module size was scaled up tenfold from approx. 40 cm to 4 m. This drastic increase in size allowed for a higher relative precision of fabrication and more reliable conclusions about the accuracy of the Finite Element Modelling (FEM) calculations. It was now possible to study the impact of self-weight and other material properties on the overall structural system. The tension forces and deflection could be accurately measured within the structure. The 2 x 2 system produces four identical corner modules. The arch-length and connection points were adjusted to create a point-symmetric suspension for the membranes.

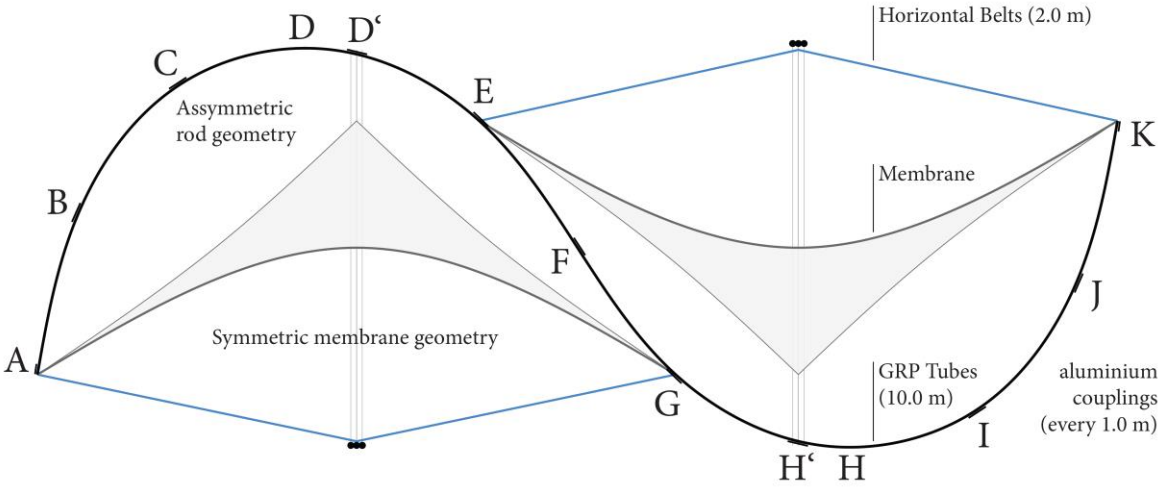

Figure 4: Section of 2 x 2 system with bending rod and couplings A-K

However, the increase in size bound to cause negative effects on the structural behavior:

- *“[...] it was shown that the scaling of bending-active structures is dependent on the significance of dead load and the influence of residual stress on stability. As an important influence on the stability, it was shown that residual compression stresses are destabilizing [...] and tension stresses are stabilizing due to nonlinear stress-stiffening effects.”* 3 (Page 185)

  Due to the inherent compression of the tensegrity struts, and the close relationship of

self-weight and bending-shape, an increase in relative deflection was to be expected.
- Each membrane is tensioned by two relatively flexible edge points. Thus, the tension is limited by the potential bending stresses inside those edge-rods.

The following provisions were taken to respond to the effects of scaling:
- To reduce the weight of the structure, glass-fiber reinforced plastic (GRP) rods, lightweight membranes (Type 1) [2] and polyester belts were chosen for construction.
- The GRP-rods were assembled in bundles of three to enhance the cumulative moment of inertia (IY) and increase the pre-tension-force along the edges.
- Each threefold parallel bundle was rigidly joined at regular intervals, like a Vierendeel girder. This limited their relative displacement and significantly increased their moment of inertia (IZ) in the horizontal direction.

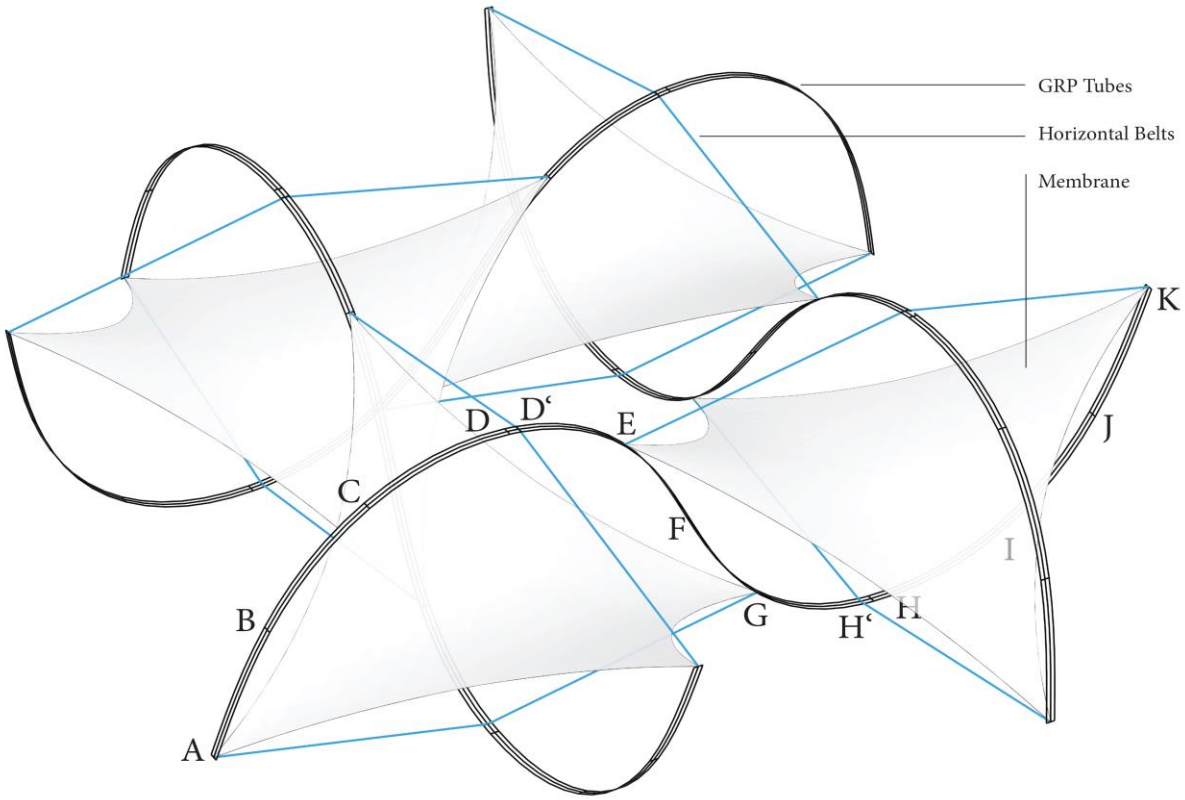

Figure 5: Bending-Activated Tensegrity system of 2 x 2 identical modules

4 PROCEDURAL METHOD

The new system requirements were verified in a physical model scaled 1:10. The following predefinitions for the FEM-calculations, fabrication and assembly were made (Figs. 4, 5):

- Four linear, elastic bundles consisting of three parallel rods are prefabricated. The

bundles are 10.0 m long. They are numbered 1-4.
- The bundles are coupled every 1.0 m to form potential connection points for the tension elements. The couplings are labeled alphabetically A-K.
- The bundles are laid out to form a hash, overlapping at 90° degrees at D and H.
- The bundles are connected with horizontal belts on top and bottom. Shortening the belts to a length of 1.9 m produces the preliminary S-shaped configuration.
- At every intersection, the membranes are attached at the tangential points and extremities of the bundles (e.g. A1, K4, G1, E4). They are tensioned by releasing the horizontal belts to 2.0m.

The exact form of the structure could not be obtained at this point. It is a result of the relation of stress between rods, membranes and belts, and is determined through the FEM-simulation.

To guarantee a symmetrical arrangement of belts and membranes, and a vertically planar bending curve for the GFK-bundles, the couplings D and H are devised moveable. They will be adjusted to the boundary conditions in the course of the simulation. The final position will be labeled D' and H'.

5 MATERIAL TESTS

Several physical tests were performed throughout the planning process. The investigation covered the material properties of GRP rods, their behavior during failure and possible plasticization. The minimal bending radii of GRP-profiles were theoretically verified.

Table 1: Table of material properties provided by Fibrolux [1]

	GRP profiles type MR mat/roving reinforced		GRP profiles type UD roving reinforced
	Z	X	Z
tensile strength	250 MPa	30 - 80 MPa	1.000 MPa
flexural strength	250 MPa	30 - 80 MPa	1.000 MPa
E-Modulus (tensile)	23.000 MPa	8.000 MPa	40.000 MPa
E-Modulus (flexural)	25.000 MPa	9.000 Mpa	45.000 MPa
elongation	1,0 - 1,8 %		2 %
compressive strength	450 MPa	90 MPa	450 MPa
compressive modulus	1.000 MPa	4.000 MPa	30.000 MPa
density	1,9 kg/dm³		2,0 kg/dm³

Technical data of GRP Profiles can vary according to the type of fibre reinforcement, shape and wall-thickness.

5.1 Profile Types

Fibrolux produces two types of GRP-Profiles: Type UD and Type MR [1]
Type UD (Uni-Directional) refers to a purely axial direction of fibers. Profiles of this type have a higher tensile strength. The fibers are protected only by a thin layer of resin. Because of this, they are vulnerable to outside influences and have a low lateral shear resistance. An

overload of bending stress causes an abrupt failure. In this case, the fibers burst and take on a flat and wide sectional shape.

Type MR (Mat-Reinforced) refers to an axial direction of fibers, reinforced by a multidirectional perimeter mat. This mat acts as a protective layer and can absorb shear forces. In case of failure, the outer mat cracks and gives in slowly. Even though Type MR has weaker mechanical properties, it was chosen for construction to allow for more safety.

5.2 Two-Point-Bending Test

In the first test setup the GRP rods were hinged at a distance of 2.0 m inside an apparatus. By moving the restraints towards each other, pressure is applied to the GRP-profile, causing a controlled buckling. The critical buckling loads were compared with the FEM calculations. However, it turned out that under high loads, the resistance of the cable mechanism inside the apparatus caused an inaccurate load transfer. A qualitative evaluation did not follow.

After applying bending stress for approx. one week, slight plastic deformation remained in the GRP rods. A reduction of residual bending stress can thus be expected for the long-term structural behavior.

5.3 Three-Point-Bending Test

In the second setup, the GRP rods were supported horizontally at distance of l = 1175 mm. A point load was applied at mid span via a belt and measured with an interposed tension scale. The deflection f and the point load P were measured and converted to the modulus of elasticity E.

D_I = inner diameter [mm]; D_O = outer diameter [mm]; I_Y = Moment of inertia [mm^4]

$$E = \frac{P \cdot l^3}{I_Y \cdot f \cdot 48} \left[\frac{N}{mm^2}\right] \qquad \text{with} \qquad I_Y = \frac{\pi}{4} \cdot (D_O{}^4 - D_I{}^4) \ [mm^4] \qquad (1)$$

The values at low deformation (f = 100 mm) were used for the calculations. At large deformations, the relative elongation of the rod axis leads to computational discrepancies.

This test proved to be a consistent and cost-effective way to evaluate material properties without a calibrated test bench. However, inaccurate measurements of up to ±5 mm and ±1.0 N have to be accounted for.

Table 2: Results of the in house Three-Point-Bending Test

Diameters		**8**	**12**	**16**	**20**	**12|8**	**16|10**	**20|14**
M. o. inertia I_Y	mm^3	201	1018	3217	7854	817	2726	5968
Distance l	mm	1715	1715	1715	1715	1715	1715	1715
Deflection f	mm	100	100	100	100	100	100	100
Point load P	N	5	33	86	111	37	54	117
M. o. elasticity E	**N/mm^2**	**~23000**	**~31000**	**~26000**	**~14000**	**~41000**	**~20000**	**~20000**

Figure 6: Bending-Activated Tensegrity system of 2 x 2 identical modules

5.4 Four-Point-Bending Test

The final tests were conducted at the "Centrum Baustoffe und Materialprüfung" to verify the property specifications. The GRP tube 20|14 Type MR was bent three times until failure using the "Biegebank CBM" (Fig. 6).[8]

The material sample was placed between four roller bearings creating an outer span of 400 mm and two symmetrical point loads at a distance of 125 mm. The time *t*, deflection *f* and the point loads *P* were recorded. The factors k_{σ} (bending stress) and k_E (bending module of elasticity) represent the geometric conditions of this setup.

From this data, the critical stress σ_{max} and the modulus of elasticity *E* were calculated. The elasticity was determined in an approximtely linear stress range between 100 and 300 N/mm².

D_I = inner diameter [*mm*]; D_O = outer diameter [*mm*]; *W* = section modulus [mm^4]

$$E = \frac{P_{\sigma=300} - P_{\sigma=100}}{f_{\sigma=300} - f_{\sigma=100}} \cdot k_E \quad \left[\frac{N}{mm^2}\right] \qquad \sigma = N \cdot k_{\sigma} \quad \left[\frac{N}{mm^2}\right] \tag{2}$$

Table 3: Results of Four-Point-Bending Test, CBM [8]

Diameter, trial		**20|14, t1**	**20|14, t2**	**20|14, t3**
Deflection $f_{\sigma=100}$	mm	7.42	7.50	7.28
Deflection $f_{\sigma=300}$	mm	21.11	20.87	19.89
Load $P_{\sigma=100}$	N	868.30	869.10	869.90
Load $P_{\sigma=300}$	N	2604.70	2608.00	2605.50
Modulus of elasticity *E*	**N/mm²**	**21758**	**22322**	**23604**
Critical stress σ_{max}	**N/mm²**	**461.0**	**386.2**	**422,2**

When comparing the test results with the specifications, it appears probable that a safety factor (approx. 1.6) was added by the manufacturer.

Specification: $\sigma_{max} = 250$ N/mm^2
Osterminski: $\sigma_{max} \approx 420$ N/mm^2

The modulus of elasticity shows a slightly lower test result than the specifications:

Specification: $E = 25000$ N/mm^2
Osterminski: $E \approx 22500$ N/mm^2
In-house test: $E \approx 20000$ N/mm^2

The higher elasticity values of the manufacturer could originate from a different experimental setup, which did not guarantee unconstrained supports as described in the test setup.

5.5 Analysis of Bending Radii

A parallel theoretical study investigated the physical relationship between curvature κ and bending moment M of bar elements based on their bending stiffness $E \cdot I$. The curvature can be described geometrically by the reciprocal value of the bending radius r.

$$\kappa = \frac{1}{r} = \frac{M}{EI} \left[m^{-1} \right] \tag{3}$$

This relationship was used to verify rods (and tubes) carrying only bending stress. If the maximum bending stress $\sigma_{R,max}$ for their specific material is known, the minimum bending radius r_{min} can be deduced:

$$r_{\min} = \frac{EI}{M_{R,\max}} = \frac{EI}{\sigma_{R,\max} \cdot W} \left[m \right] \tag{4}$$

This calculation was used throughout the design process to quickly check bending curves and profiles for plausibility. It should be mentioned that the inherent compression is not being considered in this calculation. It also proved a practical challenge to accurately verify the minimum radius of a bent structure. A ‘geometrical safety’ was always taken into account.

The allowable stress for the GRP tube (20|14, MR) was determined by using the test results and applying a safety factor of 2.0 ($\sigma_{R,\,max} = 200$ N/mm²). To determine the minimum bending radius r_{min}, the following specifications were used:

$E = 25000$ N/mm², $I = 5968$ mm4 and $W = 597$ mm³

$$r_{\min} = \frac{25000 \frac{N}{mm^2} \cdot 5968 mm^4}{200 \frac{N}{mm^2} \cdot 597 mm^3} = 1250 mm \tag{5}$$

The structure was designed with a minimum radius of approx. $r = 1400$ mm.

6 FROM-FINDING AND FINITE ELEMENT METHOD

The process of form-finding and structural analysis was simulated in an uninterrupted mechanical description using a single modeling environment. This ensured that the structural substantial residual stresses could be traced throughout all stages of design.[3] (Page 183)

6.1 From-Finding

In conventional membrane structures with almost rigid boundaries, the interaction between the membrane and the boundaries are often neglected. In this case study, the hybrid interaction between the membrane and GRP rods are so dominant that only a holistic FEM simulation could produce the accurate information for construction and workshop planning.

The bending of the GRP rods creates internal residual stresses that are threefold important: They are essential for the verification of structural integrity, the determination of the membrane forces and for the final adjustment of the overall geometry.

The GRP rods were simulated as isotropic material using the lowest tested modulus of elasticity, E = 20000 N/mm^2.

To achieve a precise overall geometry, various stress states and different tie points were analyzed and systematically optimized. Consequentially the connection point D was moved by 84 mm to the position of D' creating minimal out-of-plane deflections of the beam elements and symmetrical horizontal loads in the membrane and cables.

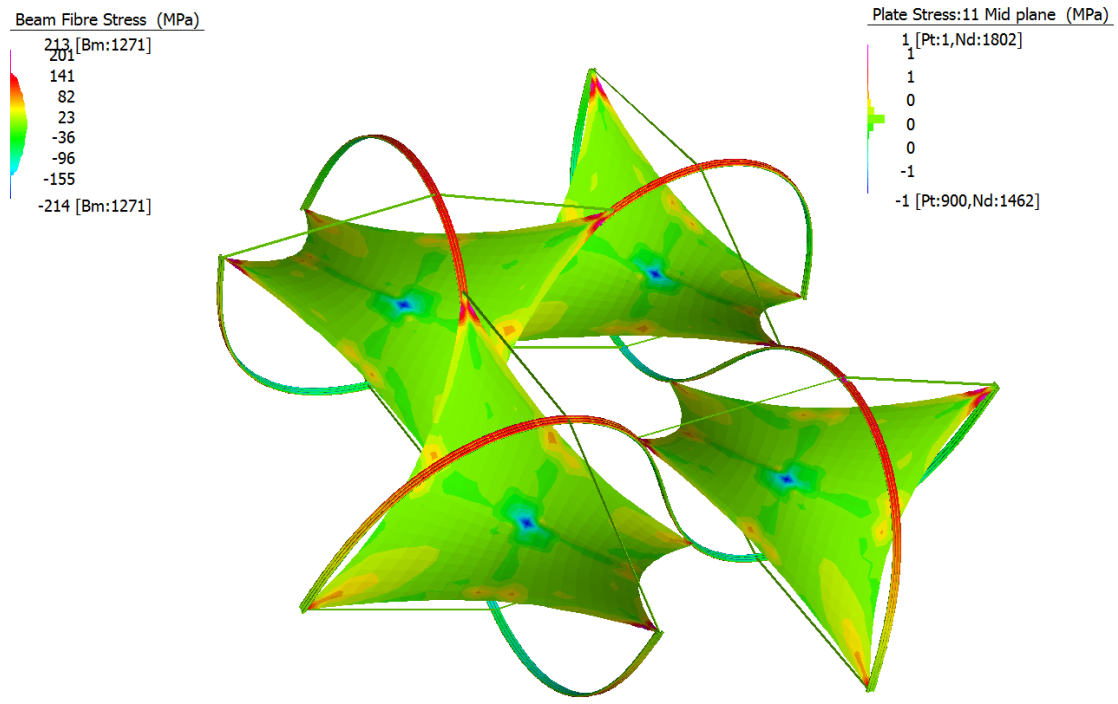

Figure 7: FEM model with stress evaluation

6.2 Structural Simulation

Using the Stage Manager of the FEM Software Strand7® PACKAGE the following incremental approach was carried out:

1. Simulation of bending by induced support displacement
2. Incorporation of tension elements with simultaneous opening and relocation of supports
3. Shortening of main tension elements
4. Adjustment of pretension
5. Incorporation of a membrane substitute cable net
6. Adjustment of pretension in all tension elements
7. Form-finding based on the shape of the membrane substitute cable net
8. Replacement of the substitute cable net by membrane elements
9. Final adjustment of pretension of the membrane and tension element
10. Transfer of the final shape of patterning and cutting algorithms

Evaluating the calculation results showed that the stress in the GRP elements were at a maximum of approx. 50% to the predefined limits of $\sigma_{max} \approx 400$ N/mm^2. The maximum residual stresses are caused by the relatively small bending radii. The FEM analysis was verified by a radius-based hand calculation.

The membrane material, which was calculated as an orthotropic shell element (without bending stiffness) is far away from its maximum capacity under the analyzed self-weight and pretensioned condition (Fig. 7). Very low wind loads were simulated in the structure. It was evident that in case of an outdoor installation, improvements of the stiffness are needed to reduce large deformations of the structure.

The coupling of the three parallel GRP-tubes was simulated by rigid link elements. The real build coupling elements were verified in an outsourced sub model with their precise dimensions and the internal forces transferred from the overall model.

6.3 Modal Analysis

The modal analysis determines the dynamic behavior of a structure and allows the detection of the most deflectable parts. It is a typical method in mechanical and earthquake engineering, and is used to find an appropriate way of stiffening.

The center points along the GRP-bundles showed large relative amplitudes at the first eigenform. They were connected by additional tension elements. As a result the structural stiffness was improved, which is equivalent to an increase of the first natural frequency.

To further improve the form-finding analysis process for future projects, the programming API of Strand7 can be used to automate the activation and deactivation of elements and support. This would allow the inclusion of optimization strategies.

7 BUILDING ELEMENTS, CONNECTIONS AND MEMBRANES

To allow repeated transportation and assembly, the exhibit was designed with reversible connection details and a maximum element dimension of 3.0 m.

7.1 Building Elements

The structure consists of the following building elements:

- 4 GRP-bundles, including 11 couplings each
- 18 tension belts
- 4 membranes

Figure 8: Cutting the GRP tubes

Figure 9: Gluing the GRP slot joints

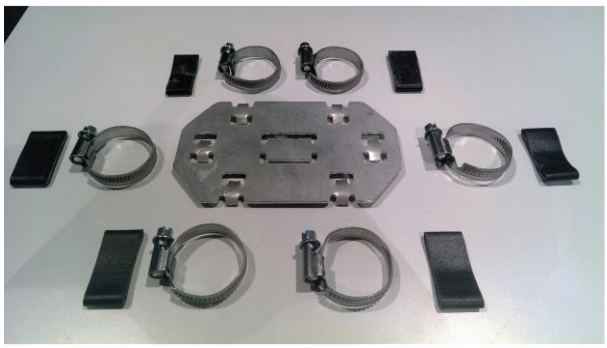

Figure10: Coupling - aluminum plate with hose clamps and rubber interlayer

7.2 Connections

The GRP-bundles form the “skeleton” of the structure, to which all other elements connect. At the couplings, all three tubes are tightened to an aluminum plate by hose clamps. The rods are protected by a rubber interlayer. This increases the friction between aluminum and fiber.

The couplings fulfill the following functions:

- Every bundle consists of three parallel tubes. They are rigidly joined by the couplings at 1.0 m intervals to produce a higher lateral bending stiffness (Fig. 10).
- The 10.0 m bundles are made up of 1.0 m, 2.0 m, and 3.0 m long tube elements. They are alternately slotted at every coupling. This slotted joint is designed as a reversible, rigid connection:

A 40 cm long GRP rod (14mm) is glued halfway into the end of one tube (Fig. 9). The projecting 20 cm rod is slotted into the subsequent tube.

- The couplings form the connection points for the tension belts and membranes. The tensile force is transmitted to the GRP tubes through friction.

7.3 Membranes

The simulation of geometry and residual stresses provided the necessary information for the form-finding of the membranes. The connector coordinates, along with the tensile force at the connection straps were read from the FEM model. This information was sent to the membrane manufacturer who produced the cutting pattern.

Two membrane materials were used: Membrane Type 1 (700g/m²) [3] and a PVC-coated mesh (approx. 600 g/m²). They were attached to the GRP tubes using polyester straps. Due to the high relative capacity of the membrane material, no additional edge strengthening was used.

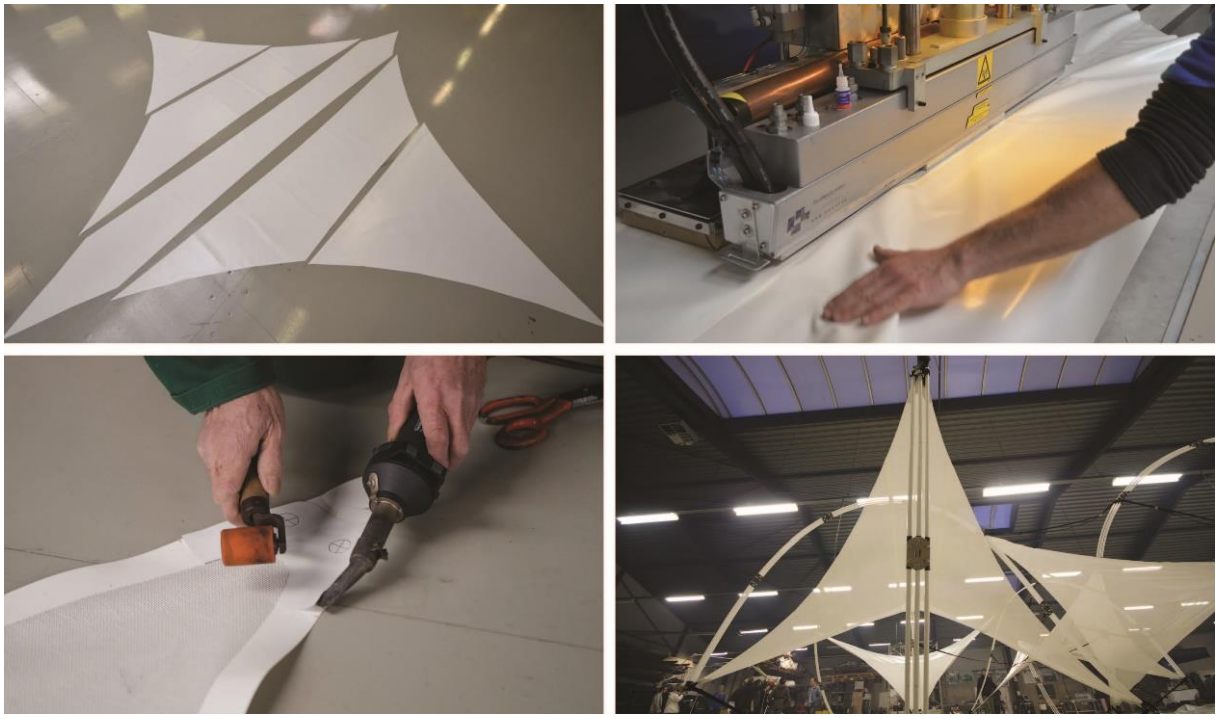

Figure11: Cutting and welding of the membranes

8 ASSEMBLY AND SAFETY MEASURES

As described in the procedural method, the bundles are laid out to form a hash and connected with the horizontal belts (Fig. 12). To avoid asymmetric construction stages, the shortening of the belts is carried out iteratively in steps of approx. 30 cm. Only after linking and tightening the membrane does the structure take its final shape. To stabilize the first eigenform (see 6.3 Modal Analysis) the centers of all four bundles are connected with two cross straps. The structure is supported vertically on its four low points.

There is a risk that the belt clamps break or are used incorrectly, causing a sudden and dangerous lash out of the GRP-bundles. All belts have therefore been equipped with a second safety clip which is continuously adjusted during the assembly. At their minimum bending radius, the GRP profiles are utilized at a maximum of 50%. In the unlikely event that one tube fails, the triple parallel arrangement will allow the deficit to be compensated by its neighboring tubes.

Figure 12: Assembly of the GRP bundles

Figure 13: Assembly test of the ‘bending-activated tensegrity’- structure

9 CONCLUSION

The structure "Form Follows Tension" combines the aesthetic and structural properties of tensegrity, membrane, and active-bending structures. This discrete structural type, "bending-activated tensegrity", is characterized by a natural, stress-informed shape, hybrid structural action and lightness.

The material properties of GRP were verified based on several bending tests. The geometry and stress distribution of the elastic structure was calculated using FEM software. The construction system was designed with reversible joints and considering measures of redundancy for a smooth and safe assembly. The closed tensegrity system holds four membranes tensioned by the bending stress of GRP tubes (Fig. 13).

In this type of structure the scale of the system plays a crucial role in the relationship between residual stress and weight. To enhance rigidity, the GRP bending rods were arranged parallel in sets of three, increasing the residual bending stress and creating an additional horizontal stiffness. For outside applications, further reduction of deformations under wind loads would be required.

Further research will include studies on practical applications of this structural type as well as further investigations of the hybrid structural action between the membrane and elastic components.

10 ACKNOWLEDGEMENT

The authors would like to thank Harry Buskes and his colleagues from CARPRO for their substantial support in fabricating the membranes for this structure. The same gratitude goes out to FIBROLUX, represented by Lisa May, for their sponsorship of materials and knowledge of the GRP-Profiles.

Many thanks to all other supporters:

- Technische Universität München
- Centrum Baustoffe und Materialprüfung, Kai Osterminski
- Gurtshop, H.R. Rathgeber GmbH&Co KG, Herbrechtlingen
- Alu Leitl, München

REFERENCES

[1] Fibrolux GmbH, http://fibrolux.com/main/knowledge, 10.04.2014

[2] Forster B. and Mollaert M., *European Design Guide for Tensile Surface Structures*, TensiNet, 2004.

[3] Lienhard J., *Bending-Active Structures*, Institut für Tragkonstruktionen und Konstruktives Entwerfen ITKE, Stuttgart, 2014.

[4] Maurin B., Motro R., Raducanu V. and Pauli N., *Soft "Tensegrity Like" Panel: Conceptual Design and Form-Finding*, IASS, 2008.

[5] Meeß-Olsohn L., *Textegrity - Textiles and Tensegrity*, LeichtBauKunst Velbert, 2004.

[6] Motro R., *Tensarch: A tensegrity double layer grid prototype*, Space Structures 5, Volume 1. Thomas Telford, London, 2002; 57.

[7] Schling E., Barthel R. and Tutsch J., *Freie Form – Experimentelle Tragstruktur*, Bautechnik 2014/12, vol 91. 2014

[8] Osterminski K., Correspondence, *Four-point-bending*, Centrum Baustoffe und Materialprüfung